2/9/99
ORIGINAL

HERMETIC PACKAGES AND FEEDTHROUGHS FOR NEURAL PROSTHESES

Quarterly Progress Report # 3

(Contract NIH-NINDS-N01-NS-8-2387)

(Contractor: The Regents of the University of Michigan)

For the Period:

October- December 1998

Submitted to the

Neural Prosthesis Program
National Institute of Neurological Disorders and Stroke
National Institutes of Health

By the

Center For Integrated Microsystems
Department of Electrical Engineering and Computer Science
University of Michigan
Ann Arbor, Michigan 48109-2122

Program Personnel:

UNIVERSITY OF MICHIGAN

Faculty:
Professor Khalil Najafi: Principal Investigator
Professor David J. Anderson, Biological Experiments

Staff:
Mr. James Wiler: Animal Implants and Surgery

Graduate Student Research Assistants:
Mr. Mehmet Dokmeci: Packaging and Accelerated Testing
Mr. Sebastien Hauvespre: Package Fabrication and Telemetry Testing

January 1998

SUMMARY

During the past quarter we continued testing of the silicon-glass packages under accelerated conditions, fully characterized a polyimide-based relative humidity sensor, made preliminary experiments with gold-silicon eutectic bonding, and made progress in remote monitoring of humidity inside the glass packages using telemetry .

Our most significant package testing results to date are those obtained from a series of silicon-glass packages that have been soaking in DI water at 85°C and 95°C for more than 4 years. We reported in the last progress reports that only 2 packages soaking at 85°C remained dry. These 2 failed during this quarter, thus concluding this study. Of the original 10 packages, the longest going sample reached a maximum of 1568 days at 85°C and 484 days at 95°C. If we assume that all of the packages at 85°C failed the same time that the 95°C packages failed, we can calculate a worst case mean time to failure of 258 days for the samples at 85°C, and of 119 days for the samples soaking at 95°C. The worst case MTTF at body temperature based on these tests is then calculated to be 58 years. These tests have been very encouraging and clearly indicate the packages can last for many years in water. We also have had 4 packages soaking at room temperature in saline. The longest lasting package has been soaking for 1468 days, and an average soak period of 1200 days at room temperature. We will continue to observe these packages for any sign of leakage. A new set of package tests had also been initiated a year ago at 85 and 95°C. At each temperature, eight packages, that had been coated with silicone rubber to prevent premature dissolution of the top polysilicon bonding layer, were soaked. These tests have provided a MTTF of 217 days at 85°C, and 125 days at 95°C, and these results indicate again the problem we have had with the dissolution of the polysilicon film. However, these results also show that the silicone coating significantly increases the time to failure of these coated packages.

Extensive tests have been performed to characterize the polyimide thin film relative humidity sensor. This relative humidity sensor not only withstands the anodic bonding process parameters, but also shows very little drift at body temperature. More fabrication and characterizations have been made this past quarter, which confirm that the sensor meets all of our requirements well and will be used to monitor humidity inside silicon-glass packages in actual animal experiments, as well as in in-vitro studies.

A new and seemingly successful approach has been studied in using telemetry to monitor the humidity inside the package. It consists of a sensing system inductively coupled to an antenna. The sensing system consists of a coil, integrated or discrete, attached to the humidity sensor described above; the antenna monitors the resonance frequency change of the sensor, which depends on the humidity. This remote monitoring of humidity will be implemented in the coming quarter.

1. INTRODUCTION

This project aims at the development of hermetic, biocompatible micropackages and feedthroughs for use in a variety of implantable neural prostheses for sensory and motor handicapped individuals. In addition, it will also develop a telemetry system for monitoring package humidity in unrestrained animals, and of telemetry electronics and packaging for stimulation of peripheral nerves. The primary objectives of the proposed research are: 1) the development and characterization of hermetic packages for miniature, silicon-based, implantable neural prostheses designed to interface with the nervous system for many decades; 2) the development of techniques for providing multiple sealed feedthroughs for the hermetic package; 3) the development of custom-designed packages and systems used in several different chronic stimulation or recording applications in the central or peripheral nervous systems in collaboration and cooperation with groups actively involved in developing such systems; and 4) establishing the functionality and biocompatibility of these custom-designed packages in *in-vivo* applications. Although the proposed research is focused on the development of the package and feedthroughs, it also aims at the development of inductively powered systems that can be used in many implantable recording and stimulation devices in general, and of multichannel microstimulators for functional neuromuscular stimulation, and multichannel recording microprobes for CNS applications in particular.

Our group here at the Center for Integrated Sensors and Circuits at the University of Michigan has been involved in the development of silicon-based multichannel recording and stimulating microprobes for use in the central and peripheral nervous systems. More specifically, during the past three contract periods dealing with the development of a single-channel inductively powered microstimulator, our research and development program has made considerable progress in a number of areas related to the above goals. A hermetic packaging technique based on electrostatic bonding of a custom-made glass capsule and a supporting silicon substrate has been developed and has been shown to be hermetic for a period of at least a few decades in salt water environments. This technique allows the transfer of multiple interconnect leads between electronic circuitry and hybrid components located in the sealed interior of the capsule and electrodes located outside of the capsule. The glass capsule can be fabricated using a variety of materials and can be made to have arbitrary dimensions as small as 1.8mm in diameter. A multiple sealed feedthrough technology has been developed that allows the transfer of electrical signals through polysilicon conductor lines located on a silicon support substrate. Many feedthroughs can be fabricated in a small area. The packaging and feedthrough techniques utilize biocompatible materials and can be integrated with a variety of micromachined silicon structures.

The general requirements of the hermetic packages and feedthroughs to be developed under this project are summarized in Table 1. Under this project we will concentrate our efforts to satisfy these requirements and to achieve the goals outlined above. There are a variety of neural prostheses used in different applications, each having different requirements for the package, the feedthroughs, and the particular system application. The overall goal of the program is to develop a miniature hermetic package that can seal a variety of electronic components such as capacitors and coils, and integrated circuits and sensors (in particular electrodes) used in neural prostheses. Although the applications are different, it is possible to identify a number of common requirements in all of these applications in addition to those requirements listed in Table 1. The packaging and feedthrough technology should be capable of:

1- protecting non-planar electronic components such as capacitors and coils, which typically have large dimensions of about a few millimeters, without damaging them;
2- protecting circuit chips that are either integrated monolithically or attached in a hybrid fashion with the substrate that supports the sensors used in the implant;
2 interfacing with structures that contain either thin-film silicon microelectrodes or conventional microelectrodes that are attached to the structure;

Table 1: General Requirements for Miniature Hermetic Packages and Feedthroughs for Neural Prostheses Applications

Package Lifetime:

≥ 40 Years in Biological Environments @ 37°C

Packaging Temperature:

≤360°C

Package Volume:

10-100 cubic millimeters

Package Material:

Biocompatible
Transparent to Light
Transparent to RF Signals

Package Technology:

Batch Manufactureable

Package Testability:

Capable of Remote Monitoring
In-Situ Sensors (Humidity & Others)

Feedthroughs:

At Least 12 with ≤125μm Pitch
Compatible with Integrated or Hybrid Microelectrodes
Sealed Against Leakage

Testing Protocols:

In-Vitro Under Accelerated Conditions
In-Vivo in Chronic Recording/Stimulation Applications

We have identified two general categories of packages that need to be developed for implantable neural prostheses. The first deals with those systems that contain large components like capacitors, coils, and perhaps hybrid integrated circuit chips. The second deals with those systems that contain only integrated circuit chips that are either integrated in the substrate or are attached in a hybrid fashion to the system.

Figure 1 shows our general proposed approach for the package required in the first category. This figure shows top and cross-sectional views of our proposed approach here. The package is a glass capsule that is electrostatically sealed to a support silicon substrate. Inside the glass capsule are housed all of the necessary components for the system. The electronic circuitry needed for any analog or digital circuit functions is either fabricated on a separate circuit chip that is hybrid mounted on the silicon substrate and electrically connected to the silicon substrate, or integrated monolithically in the support silicon substrate itself. The attachment of the hybrid IC chip to the silicon substrate can be performed using a number of different technologies such as simple wire bonding between pads located on each substrate, or using more sophisticated techniques such as flip-chip solder reflow or tab bonding. The larger capacitor or microcoil components are mounted on either the substrate or the IC chip using appropriate epoxies or solders. This completes the assembly of the electronic components of the system and it should be possible to test the system electronically at this point before the package is completed. After testing, the system is packaged by placing the glass capsule over the entire system and bonding it to the silicon substrate using an electrostatic sealing process. The cavity inside the glass package is now hermetically sealed against the outside environment. Feedthroughs to the outside world are provided using the grid-feedthrough technique discussed in previous reports. These feedthroughs transfer the electrical signals between the electronics inside the package and various elements outside of the package. If the package has to interface with conventional microelectrodes, these microelectrodes can be attached to bonding pads located outside of the package; the bond junctions will have to be protected from the external environment using various polymeric encapsulants. If the package has to interface with on-chip electrodes, it can do so by integrating the electrode on the silicon support substrate. Interconnection is simply achieved using on-chip polysilicon conductors that make the feedthroughs themselves. If the package has to interface with remotely located recording or stimulating electrodes that are attached to the package using a silicon ribbon cable, it can do so by integrating the cable and the electrodes again with the silicon support substrate that houses the package and the electronic components within it.

Figure 2 shows our proposed approach to package development for the second category of applications. In these applications, there are no large components such as capacitors and coils. The only component that needs to be hermetically protected is the electronic circuitry. This circuitry is either monolithically fabricated in the silicon substrate that supports the electrodes (similar to the active multichannel probes being developed by the Michigan group), or is hybrid attached to the silicon substrate that supports the electrodes (like the passive probes being developed by the Michigan group). In both of these cases the package is again another glass capsule that is electrostatically sealed to the silicon substrate. Notice that in this case, the glass package need not be a high profile capsule, but rather it need only have a cavity that is deep enough to allow for the silicon chip to reside within it. Note that although the silicon IC chip is originally 500μm thick, it can be thinned down to about 100μm, or can be recessed in a cavity created in the silicon substrate itself. In either case, the recess in the glass is less than 100μm deep (as opposed to several millimeters for the glass capsule). Such a glass package can be easily fabricated in a batch process from a larger glass wafer.

The above two approaches address the needs for most implantable neural prostheses. Note that both of these techniques utilize a silicon substrate as the supporting base, and are not directly applicable to structures that use other materials such as ceramics or metals. Although this may seem a limitation at first, we believe that the use of silicon is, in fact, an advantage because it is biocompatible and many emerging systems use silicon as a support substrate.

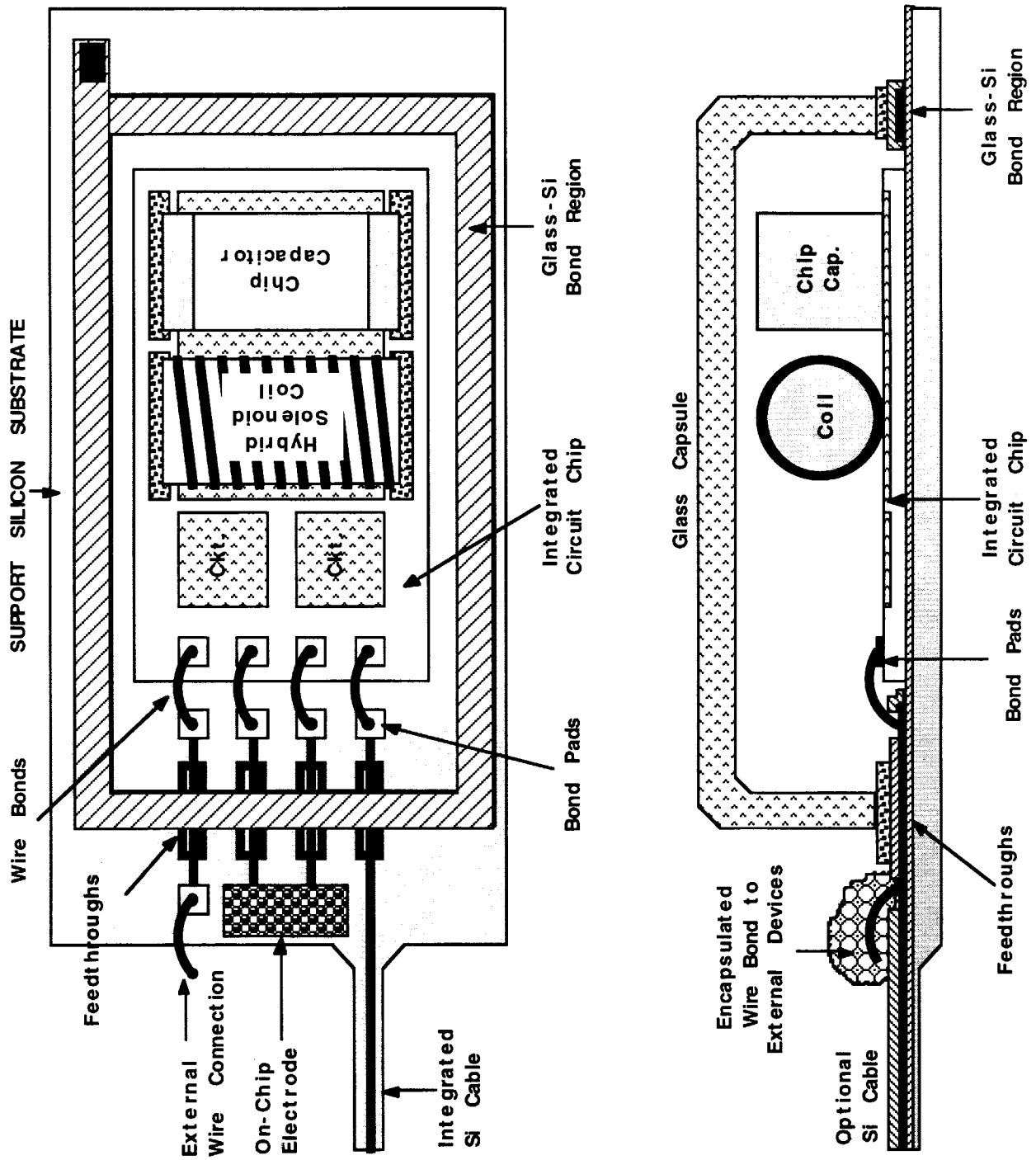

Figure 1: A generic approach for packaging implantable neural prostheses that contain a variety of components such as chip capacitors, microcoils, and integrated circuit chips. This packaging approach allows for connecting to a variety of electrodes.

We will further improve the silicon glass package and its built-in feedthroughs, and will study and explore alternative technologies for hermetic packaging of implantable systems. In particular, we have proposed using a silicon capsule that can be electrostatically bonded to a silicon substrate thus allowing the capsule to be machined down to dimensions below a 100μm. We will also develop an implantable telemetry system for monitoring package humidity in unrestrained animals for a period of at least one year. Two separate systems have been proposed, one based on a simple oscillator, and the other based on a switched-capacitor readout interface circuit and an on-chip low-power AD converter, both using a polyimide-based humidity sensor. This second system will telemeter the humidity information to an outside receiver using a 300MHz on-chip transmitter.

Finally, we have forged potential collaborations with two groups working in the development of recording/stimulating systems for neural prostheses. The first group is that led by Professor Ken Wise at the University of Michigan, which has been involved in the development of miniature, silicon-based multichannel recording and stimulation system for the CNS for many years. Through this collaboration we intend to develop hermetic packages and feedthroughs for a 3-D recording/stimulation system that is under development at Michigan. We will also develop the telemetry front end necessary to deliver power and data to this system. The second group is at Case Western Reserve University, led by Prof. D. Durand, and has been involved in recording and stimulation from peripheral nerves using cuff electrodes. Through this collaboration we intend to develop a fully-integrated, low-profile, multichannel, hermetic, wireless peripheral nerve stimulator that can be used with their nerve cuff electrode. This system can be directly used with other nerve cuffs that a number of other groups around the country have developed. Both of these collaborations should provide us with significant data on the reliability and biocompatibility of the package.

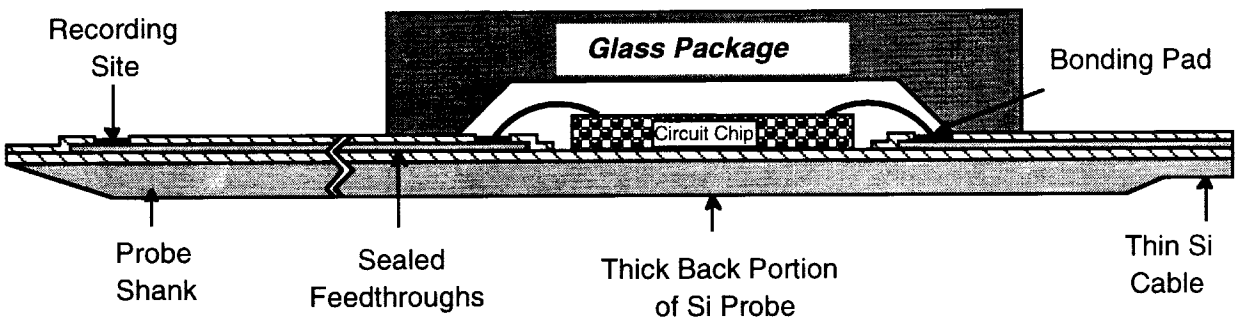

Figure 2: Proposed packaging approach for implantable neural prostheses that contain electronic circuitry, either monolithically fabricated in the probe substrate or hybrid attached to the silicon substrate containing microelectrodes.

2. ACTIVITIES DURING THE PAST QUARTER

2.1 Hermetic Packaging

Over the past few years we have developed a biocompatible hermetic package with high density multiple feedthroughs. This technology utilizes electrostatic bonding of a custom-made glass capsule to a silicon substrate to form a hermetically sealed cavity, as shown in Figure 3. Feedthrough lines are obtained by forming closely spaced polysilicon lines and planarizing them with LTO and PSG. The PSG is reflowed in steam at 1100°C for 2 hours to form a planarized surface. A passivation layer of oxide/nitride/oxide is then deposited on top to prevent direct exposure of PSG to moisture. A layer of fine-grain polysilicon (surface roughness 50Å rms) is deposited and doped to act as the bonding surface. Finally, a glass capsule is bonded to this top polysilicon layer by applying a voltage of 2000V between the two for 10 minutes at 320 to 340°C, a temperature compatible with most hybrid components. The glass capsule can be either custom molded from Corning code #7740 glass, or can be batch fabricated using ultrasonic micromachining of #7740 glass wafers.

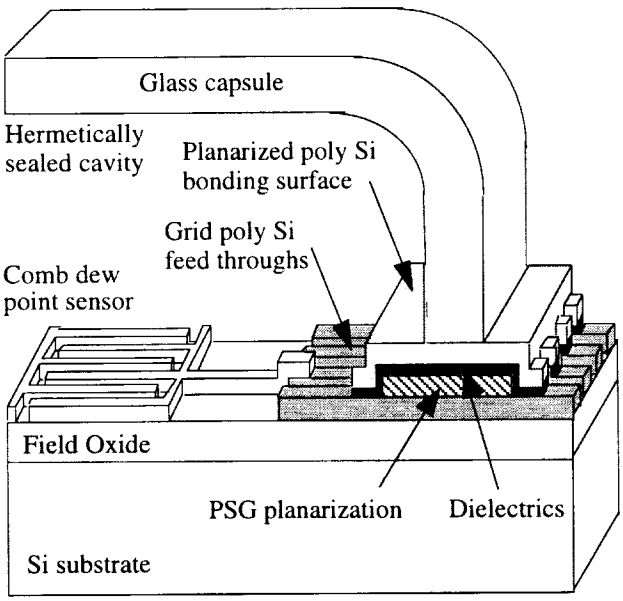

Figure 3: The structure of the hermetic package with grid feedthroughs.

During the past few years we have electrostatically bonded and soak tested over one hundred and sixty of these packages. The bonding yield is about 82% (yield is defined as the percentage of packages which last more than 24 hours in the solution they are soaked in). We should also mention that the earlier tests that have been going for more than 4 years (room temperature soak tests in saline and the 85°C and the 95°C tests in deionized water) have been made with silicon substrates that are thinned (~150μm) and bonded to the custom molded glass capsules. All of the most recent tests (85°C and 95°C tests in saline, as well as silicone rubber coated devices) were performed with the silicon substrates having full thickness (~500μm) and bonded to the ultrasonically machined glass capsules with a flat top surface. This quarter we concluded the soak tests in de-ionized water after more than 4 years at 85° C, and in saline at room temperature for over 4 years. The ongoing room temperature tests and the concluded high temperature DI water tests are detailed in the following sections.

2.1.1 Accelerated Soak Tests in Deionized Water

This quarter, we continued and concluded the accelerated soak tests in DI water. After being soaked at 85°C for more than 4 years, the last two packages which remained at the beginning of the quarter, without showing any sign of moisture inside the package, have failed. For one of the packages, the substrate, which seemed not to have been etched so far, was found almost entirely dissolved in less than a month, except for a thin transparent layer on which some metal layer is still attached, and for a thin remaining film on the bonding area of the glass capsule. The other package was found with the substrate totally separated from the glass capsule, with no remaining layer attached on the glass.

These 2 devices were the last remaining of 20 devices, which were soaked at high temperature. High temperature is the parameter chosen as the acceleration factor, as it is easy to control and accelerate exponentially diffusion of moisture. Ten samples were soaked at 85°C and 10 others at 95°C. Failure is defined as the room temperature condensation of moisture inside the package. The testing sequence for these packages started by cooling the sample to room temperature from its soak bath at the elevated temperature. The samples were next rinsed with deionized water and then carefully dried with a nitrogen gun. We then measured the impedance of the dew point sensors and inspect the sample carefully for leakage under the microscope. A significant change in impedance (about 2 orders of magnitude) and observation of visible condensation inside the package would both be classified as the failure of the package under test. Tables 2 and 3 below list some pertinent data from these soak tests. Figure 4 summarizes the final results from the 95°C soak tests and Figure 5 summarizes the results obtained so far from the 85°C tests. These figures also list the causes of failure for individual packages when it is known, and they show a curve fit to our lifetime data to illustrate the general trend.

Of the original 10 samples in the 95°C tests, the longest lasting package survived for a total of 484 days. The calculated mean time to failure of these packages is 135.7 days excluding the handling errors. Of the original 10 packages in the 85°C soak tests, the longest lasting package survived for a total of 1568 days. The calculated mean time to failure of these packages is 1115 days excluding the handling errors.

Table 2: Key data for 95°C soak tests in DI water.

Number of packages in this study	10
Soaking solution	DI water
Failed within 24 hours (not included in MTTF)	1
Packages lost due to mishandling	2
Longest lasting packages in this study	484 days
Packages still under tests with no measurable room temperature condensation inside	0
Average lifetime to date (MTTF) including losses due to mishandling	*118.7 days*
Average lifetime to date (MTTF) not including losses due to mishandling	*135.7 days*

Table 3: Key data for 85°C soak tests in DI water.

Number of packages in this study	10
Soaking solution	DI water
Failed within 24 hours (not included in MTTF)	2
Packages lost due to mishandling	3
Longest lasting packages so far in this study	1568 days
Packages still under tests with no measurable room temperature condensation inside	0
Average lifetime to date (MTTF) including losses due to mishandling	*707 days*
Average lifetime to date (MTTF) not including losses due to mishandling	*1115 days*

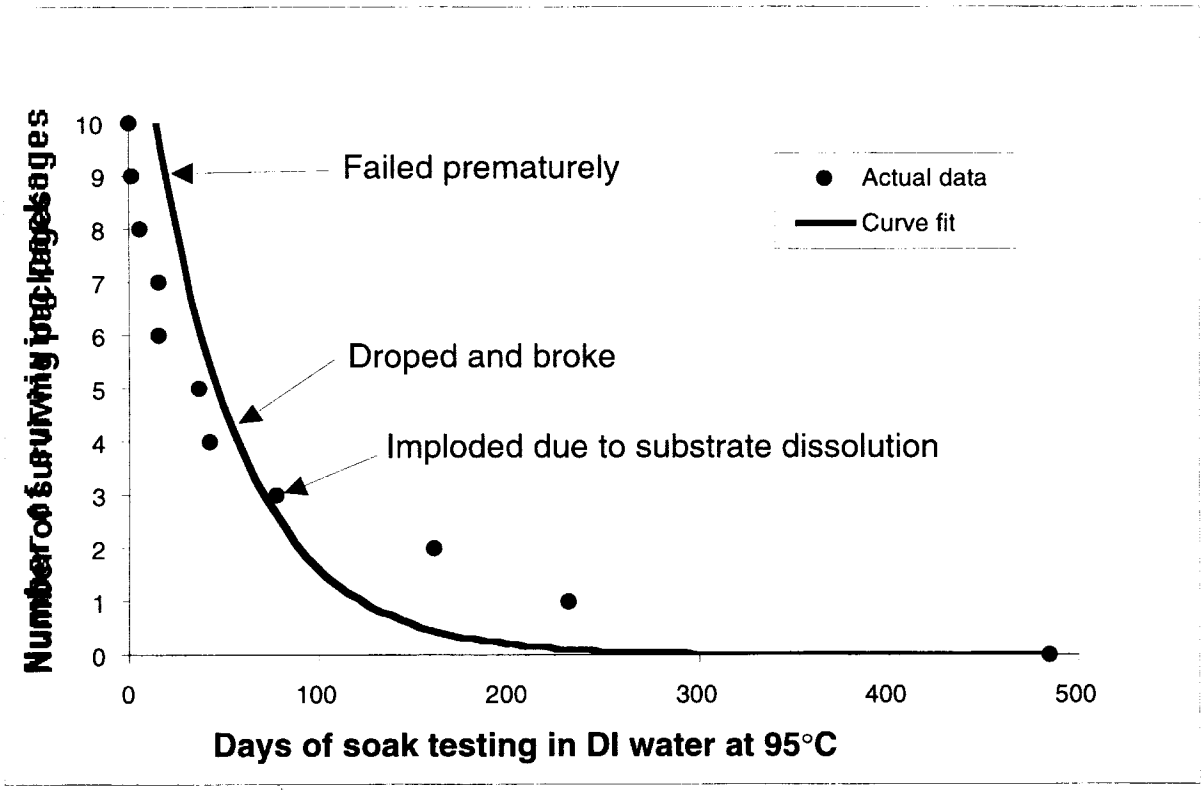

Figure 4: Summary of the lifetimes of the 10 packages that have been soak tested at 95°C in DI water.

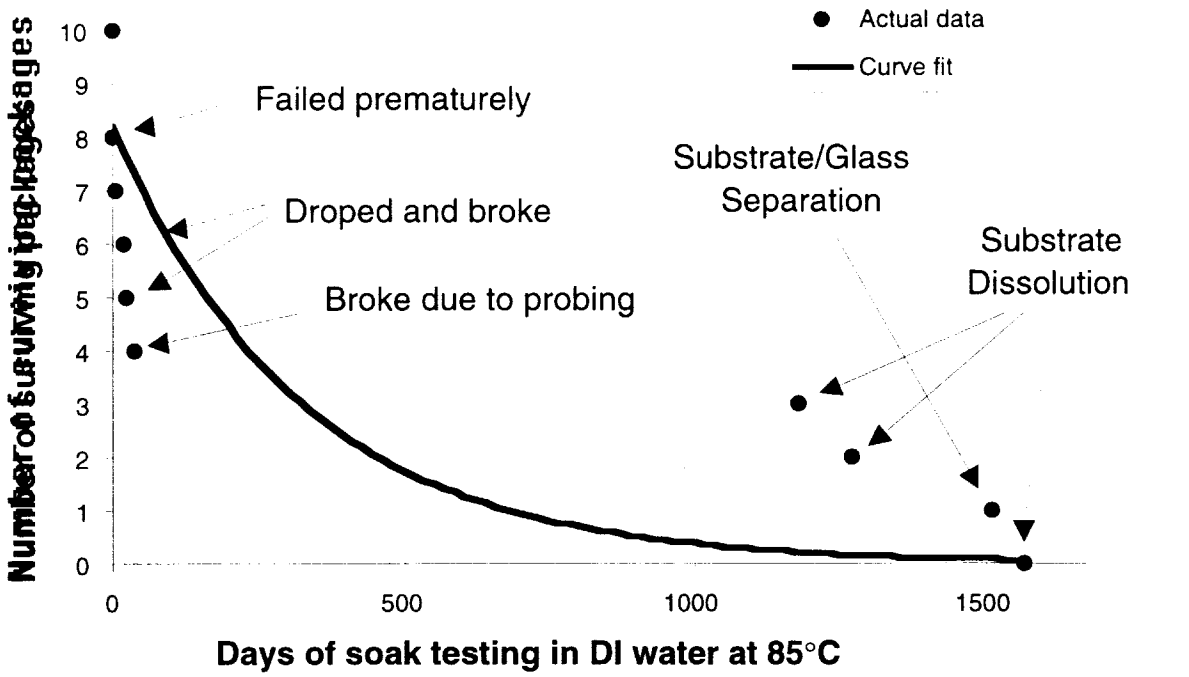

Figure 5: Summary of the lifetimes of the 10 packages that have been soak tested at 85°C in DI water.

2.1.2 Interpretation of Soak Test Results in Deionized Water

Generally during accelerated testing, one models the mean time to failure (MTTF) as an Arrhenius processes (In the VLSI industry this model is used for failure due to diffusion, corrosion, mechanical stress, electromigration, contact failure, dielectric breakdown, and mobile ion/surface inversion). The generalized equation used in all these cases is given below where MTTF is the mean time to failure, A is a constant, ξ is the stress factor other than temperature, (such as pressure or relative humidity), n is the stress dependence, Q is the activation energy, K_B is Boltzman's constant, and T is the temperature in Kelvin.

$$MTTF = A \cdot \xi^{-n} \cdot e^{\left(\frac{Q}{K_B T}\right)}$$

For the accelerated soak tests that we have performed on the packages, there was no stressing factor other than temperature, so the ξ term drops out of the above equation. The resulting equation can be rewritten as a ratio of MTTFs as it is below.

$$AF = \frac{MTTF_{Normal}}{MTTF_{Accelerated}} = e^{\frac{Q}{K_B}\left(\frac{1}{T_{Normal}} - \frac{1}{T_{Accelerated}}\right)}$$

By using these MTTFs at 85°C and 95°C, we can easily calculate the activation energy (Q) and from this activation energy we can proceed to obtain an acceleration factor (AF) for these tests, and then calculate the MTTF at the body temperature. Moreover, after analyzing our failed samples we have found out and mentioned in the past progress reports that some of the samples at the 95°C tests have failed prematurely due to the enhanced dissolution rate for silicon at this temperature. Since the dissolution reaction is an exponential function of temperature, the samples at the 85°C tests have been effected less than the ones at 95°C. The model we use only accounts for acceleration of moisture diffusion, but not dissolution. We will still keep and update the data for the tests performed at 85°C. Moreover, for our calculations we assume that all the samples in the 85°C tests have also failed the same time as the longest going sample in the 95°C tests and proceed with the calculations as follows:

$$MTTF|_{85°C} = 257.6\,Days \quad MTTF|_{95°C} = 118.7\,Days$$

Q=0.88 eV, AF(95°C)=179.5, AF(85°C)=82.7

$$MTTF|_{37°C} = 58.4\,Years$$

We should also note that we have included every single sample in the 85°C and 95°C soak tests in this calculation except the 15% that failed during the first day (we assume that these early failures can be screened for). Moreover, some of these capsules have failed due to mishandling during testing rather than due to actual leakage into the package. If we disregard the samples that we have attributed failure due to mishandling we obtain a longer mean time to failure:

$$MTTF|_{85°C} = 396\,Days \quad MTTF|_{95°C} = 136\,Days$$

Q=1.217 eV, AF(95°C)=1304, AF(85°C)=447

$$MTTF|_{37°C} = 485\,Years$$

2.1.3 Ongoing Room Temperature Soak Tests in Saline

The packages soaked in saline at room temperature have been under test for more than 4 years now. These soak tests were originally started as a complement to the accelerated soak tests at the higher temperatures. We have consistently observed in these tests that at room temperature we are below the activation energy required to cause dissolution and hence we have not yet observed any dissolution related failures. This result is in accordance with the acceleration model used in interpreting the high temperature tests. Indeed, it seems to confirm that the activation energy for the dissolution of the substrate or the top polysilicon is high. Thus, if the dissolution has an effect at high temperature, it may not be significant at body temperature, because of an exponential decrease of the acceleration factor with temperature.

Out of the original 6 packages, one failed prematurely the first day and one failed because of mishandling. The 4 other devices are still under test and present no sign of leakage into the capsule after being soaked for 1468 days. Table 7 summarizes the data obtained from these soak tests.

Table 4: Data for room temperature soak tests in saline.

Number of packages in this study	6
Soaking solution	Saline
Failed within 24 hours (not included in MTTF)	1
Packages lost due to mishandling	1
Longest lasting packages in this study	1468 days
Packages still under tests with no measurable room temperature condensation inside	4
Average lifetime to date (MTTF) so far including losses due to mishandling	1199.2 days
Average lifetime to date (MTTF) so far not including losses due to mishandling	1468 days

2.2 Complete Characterization of the Relative Humidity Sensor

During this past quarter, we have performed a complete characterization of the polyimide relative humidity sensor. The design, fabrication and initial results on the highly sensitive polyimide relative humidity sensor are described in a previous quarterly report. This relative humidity sensor can be utilized as a part of an active relative humidity sensing system or it can function as a part of a passive telemetric system that can record the amount of humidity inside packages implanted into animals. Table 5 summarizes both calculated and measured properties of a 1200Å thick sensor. A photograph of the fabricated device is shown in Figure 6.

Table 5: The properties of the relative humidity sensor.

Parameter	Value
Moisture Sensing Material	CU1512, Polyimide
Capacitor Plate Area	1 mm2
Effective Area	0.625 mm2
Thickness	1200 Å
Capacitance (0% RH)	152 pF
Capacitance (100% RH)	180 pF
Sensitivity (Calculated)	0.28pF /%RH
Sensitivity (Measured)	0.86pF /%RH
Drift @37°C, 50% RH	0.53% RH
Hysteresis	1.75% RH
Nonlinearity	0.6% RH

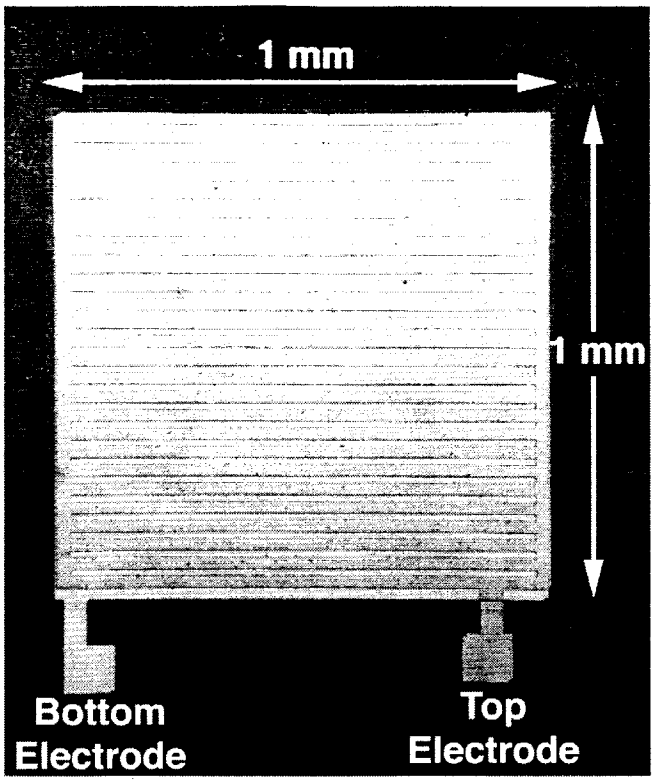

Figure 6: The photograph of the relative humidity sensor.

The sensor is wire bonded to a printed circuit board (PCB), and tested inside an environmental chamber. Since the package will be tested inside an animal host, body temperature (37°C) is used in almost all measurements. The humidity response was typically measured from 30% RH to 70% RH with increments of 10%RH. Since it normally takes ≈ 20-30 minutes for the humidity chamber to reach equilibrium, all the readings are taken 30 minutes after a humidity setting has been changed. The polyimide humidity sensors typically have a relatively fast response, 30 minutes is more than sufficient for the device to reach equilibrium. Almost all the capacitance measurements are performed at 1MHz using a HP 4280A Capacitance Meter with a resolution of 0.1pF. Sensors with various polyimide thickness are fabricated and tested inside the humidity chamber, and test results are presented below.

Sensitivity and Linearity

The reasons for the requirement of a very sensitive relative humidity sensor are twofold. First of all, high sensitivity results in large capacitance variations with which a passive telemetric monitoring unit can be realized easily. Secondly, since the variation in capacitance is large, there is no need for additional interface circuitry which otherwise would have taken additional space in the package. Linearity is also desired for the sensor since it will be easy to correlate the capacitance reading to the actual humidity inside the package. With this in mind, we have fabricated a large set of devices and measured their response to relative humidity.

The sensitivity of a parallel-plate capacitive humidity sensor is given by:

$$\frac{\Delta C}{\Delta RH} \propto \frac{A}{d}$$

where ΔC is the change in total capacitance, ΔRH is the change in relative humidity, A is the moisture absorbing area of the sensor, and d is the thickness of the polyimide film. From the equation above, as the thickness of the film is reduced, the capacitance and sensitivity increase. Furthermore, experimental results have shown that polyimide films thinner than 300Å cannot be reliably fabricated because of pinholes in the film which cause a short circuit between the two metal electrodes. Several sensors having different thickness for the polyimide film are fabricated, including a 300Å (spun at 4,000 rpm), 660Å (spun at 2,000rpm) and 1200Å (spun twice at 2,000 rpm) thick polyimide dielectric film. Figures 7 and 8 show the measured capacitance versus relative humidity for a 300Å-thick and 660Å-thick polyimide films tested at 37°C respectively.

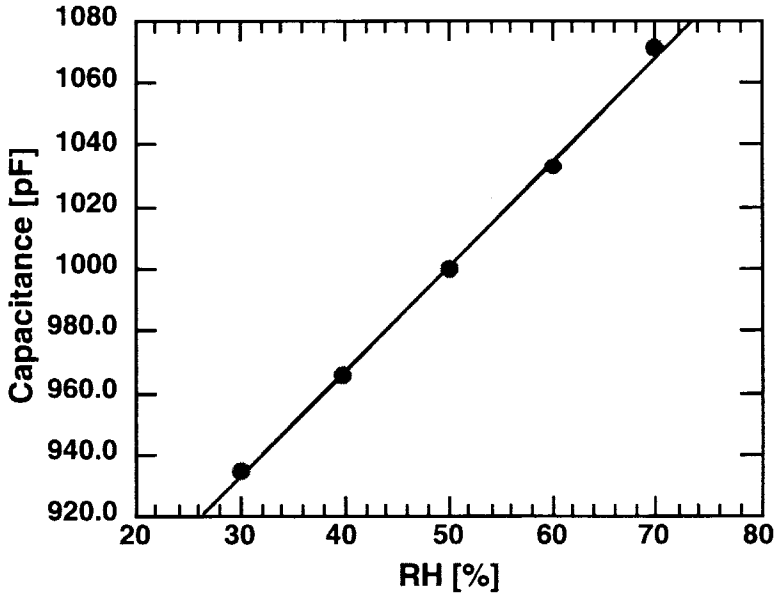

Figure 7: Measured capacitance versus relative humidity for a 300Å device at 37°C.

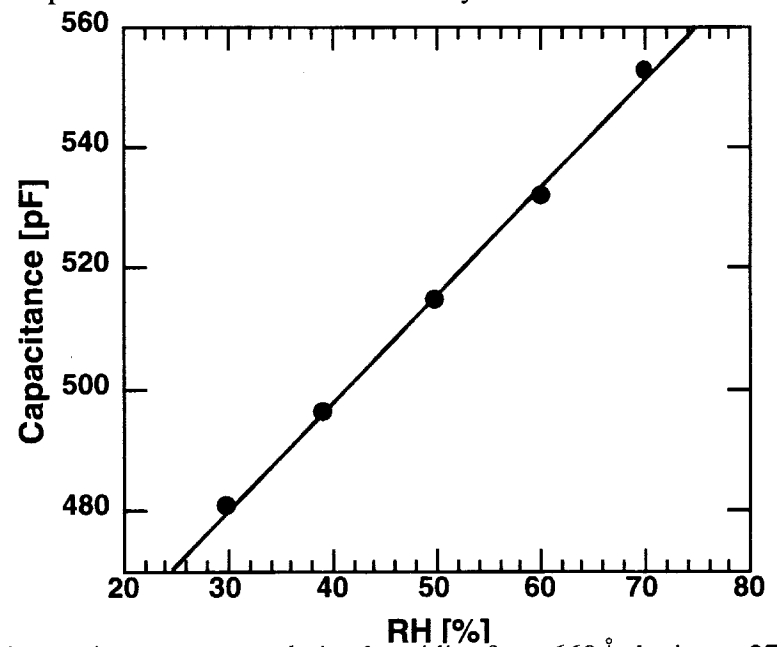

Figure 8: Measured capacitance versus relative humidity for a 660Å device at 37°C.

As seen in both figures, the response to relative humidity is fairly linear (nonlinearity is calculated to be less than 2% RH for all devices) over the full scale range of 30-70% RH. From the thinnest (300Å) device we have achieved a very high sensitivity of 3.4pF/%RH. Table 6 summarizes the measured sensitivities and nonlinearities for the three different sensor types.

Table 6: A comparison of different polyimide designs.

d(Å)	C(calc, pF)	C(meas, pF)	S(pF/%RH)	Nonlin(%RH)
298	668	1050	3.4	1.1
649	307	515	1.7	0.4
1208	165	265	0.86	0.6

Stability

Since the sensor is not accessible for calibration after it is sealed inside the glass-silicon package, it is important that it shows little or no drift. A 1200Å-thick polyimide sensor has been tested at 37°C for 48 hours at 50% RH, and another one is tested at 37°C for 48 hours at 80% RH; the results from both of these tests are shown in Figure 9. The relatively higher drift as seen in Figure 9 is a known characteristic of polyimide humidity sensors and agrees well with published results [1]. The maximum drift was approximately 0.4% RH at 50% RH conditions and was about 11.4% RH at 80% RH conditions. Since the initial sealing of the package is performed in a low humidity environment, the polyimide sensor is expected to perform satisfactorily.

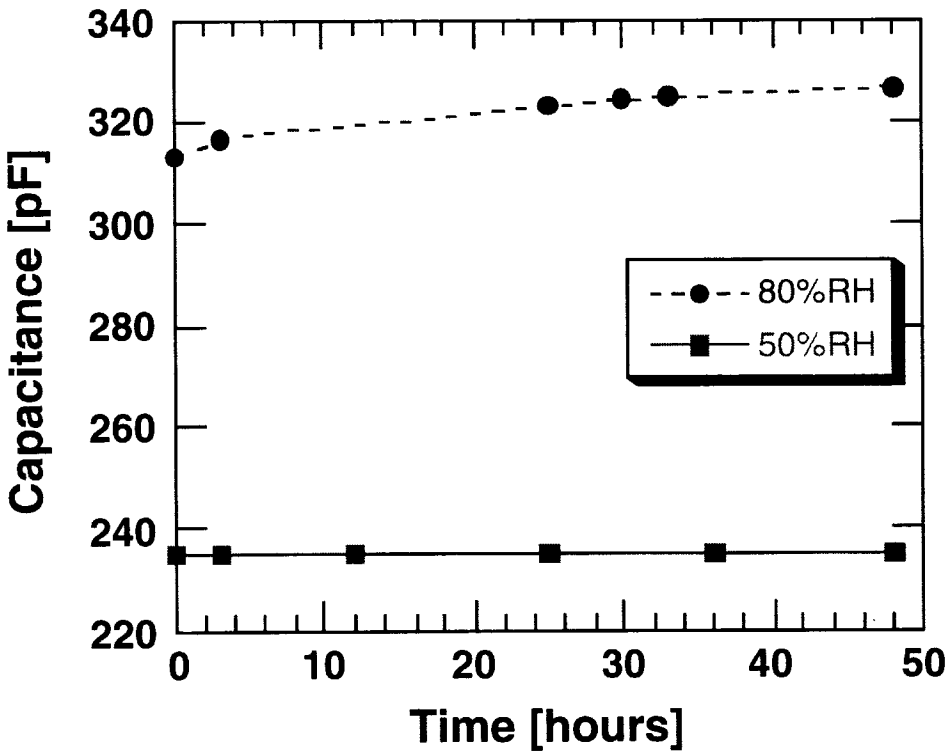

Figure 9: Stability results from a 1200Å device for 48 hours at 37°C.

Extended Range Operation

All of the measurements presented above were performed inside the humidity chamber with humidity levels ranging from 30% to 70% RH. This has been primarily due to the time it takes to perform the measurements at lower humidity levels. For instance, the minimum lower limit for the test chamber at 37°C is ≈20% and it takes a significant amount of time (on the order of days) to reach this low level. Nevertheless, to verify extended-range operation, one 1200Å device was tested for the maximum possible range determined by the humidity chamber. The measured results are shown in Figure 10. As evident, the sensor response is fairly linear and representative of previous measurements for humidity levels of up to 70% RH. One also expects that the sensors would behave linearly for humidity levels below 20% which is an area that will be investigated in the future.

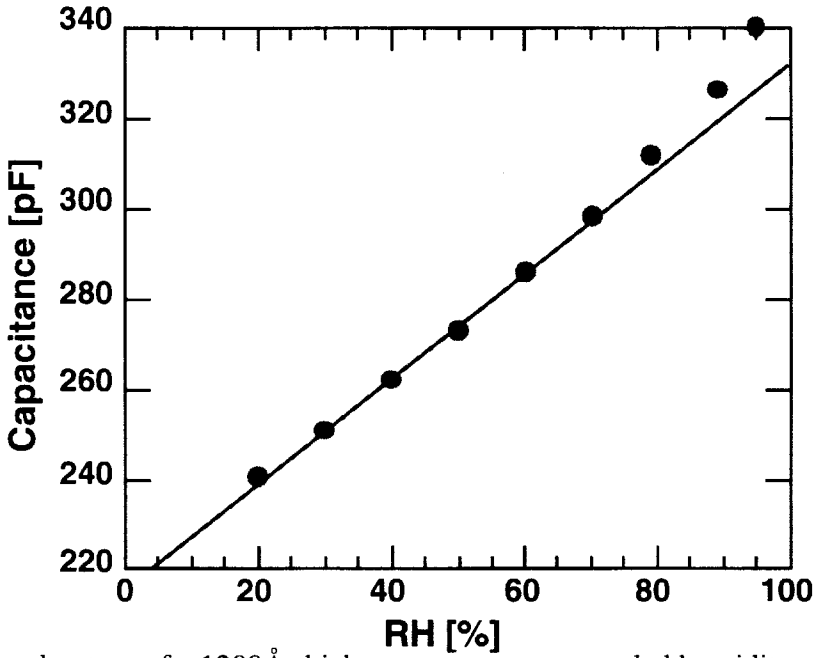

Figure 10: Measured output of a 1200Å-thick sensor over an extended humidity range.

Exposure To Anodic Bonding Process

The effect of high temperature processing after the sensors are fabricated and ready for testing has also been studied. A 1200Å-thick device has been tested inside the humidity chamber before any exposure to high temperature steps, and the sensor output is found to be linear. The device is then dismounted from the PCB, and instantly placed on a hot plate with a temperature of 400°C. After one hour at this temperature, the device is again instantly removed from the hot plate and cooled down to room temperature, mounted on the board, and tested inside the environmental chamber, and the entire process is repeated. Figure 11 shows test results for this sensor both before and after two exposures to the high temperature environment. As evident, the response is quite linear and consistent. The shift in capacitance (offset) is perhaps due to the fact that the polyimide film has been further dried and depleted of any residual moisture which may have been trapped in it during processing. After the second exposure to 400°C, we see very little change in the sensor sensitivity or offset. Out of the devices we tested from 660Å and 1200Å batch, all of them survived during the high temperature cycling step. The yield from the 300Å devices was about 70%. This loss is most likely due to aluminum diffusing through the pinholes in the polyimide at this high temperature.

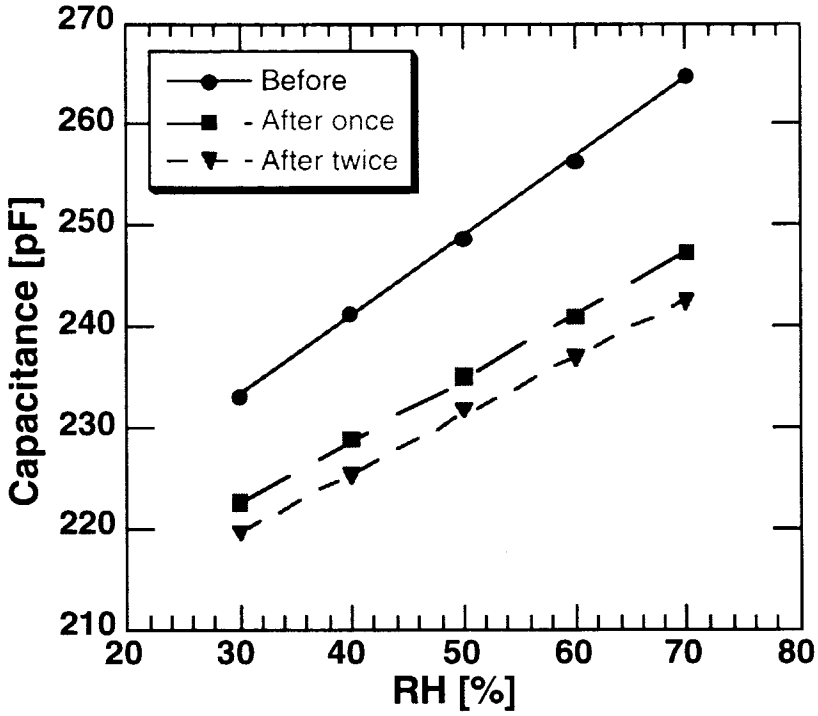

Figure 11: Measured output of a 1200Å-thick sensor before and after two bakes at a temperature of 400°C for one hour.

Response Dependence on Measurement Frequency

All previous measurements have been performed at a frequency of 1MHz. In order to determine the dependence of the response of the sensor on the frequency at which device capacitance is measured, a 660Å-thick device has been tested at 3 test frequencies (i.e., 1.1KHz, 10KHz and 100kHz), and the results are shown in Figure 12. Note that the response at each frequency is fairly linear, and the capacitance decreases with increasing frequency. At 45% RH, the capacitance is 5.6% lower at 100kHz than at 1.1kHz.

Tests On The Actual Packaging Substrate

One of the 300Å-thick relative humidity sensors was mounted on a silicon substrate and using the feedthrough leads was wire bonded to a PCB, as shown in Figure 13. This device was exposed to an ambient humidity of 30-60% RH and behave linearly independent of frequency. These results indicate that this relative humidity sensor can also replace the dew point sensor and be utilized to monitor the environment inside anodically bonded packages with more precision. Future efforts will focus on incorporating the RH sensor into the packaging substrate with a telemetry unit and performing tests in animal hosts.

Scaling the humidity sensor for other applications

A 1mm x 1mm relative humidity sensor is fabricated and tested and found to satisfy all of our requirements. In order to make this a more versatile device we have investigated the consequences of scaling the device in area and in thickness. The effects of making the device smaller. The smaller sensor would be used in smaller micropackages and also for the active humidity measurement system since it leaves more room for other components.

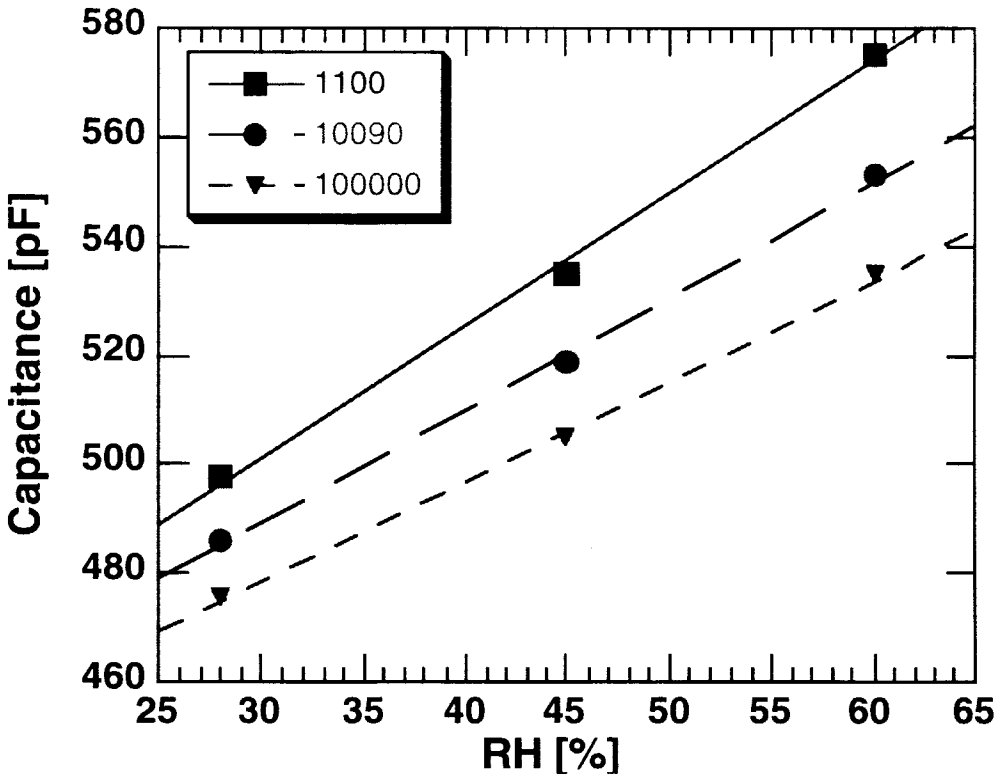

Figure 12: Measured capacitance vs. ambient RH for 3 different test frequencies for a 660Å-thick sensor.

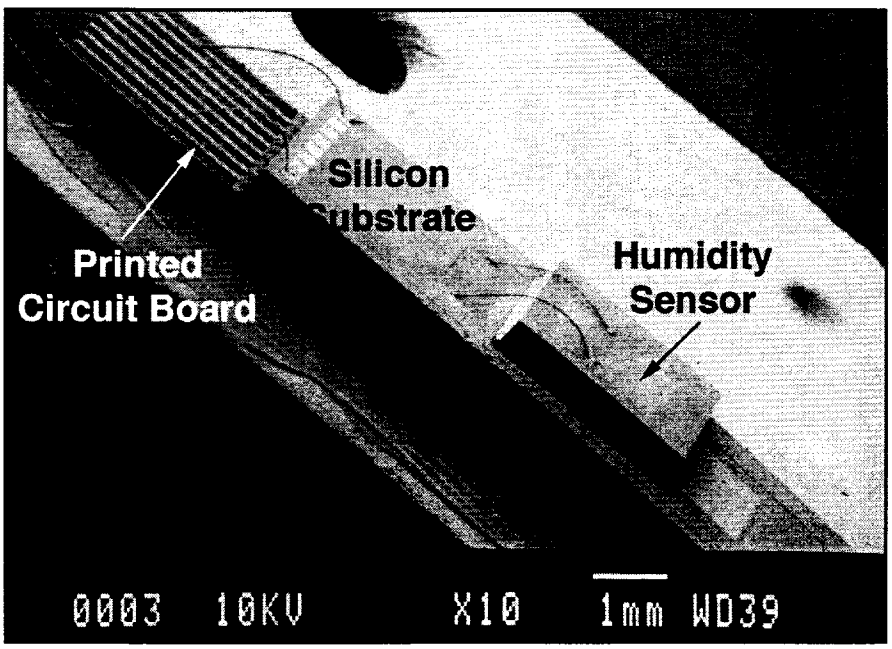

Figure 13: SEM micrograph of a RH sensor mounted on a silicon substrate for hybrid testing.

The capacitance of the humidity sensor is given by:

$$C = \frac{A\varepsilon_o\varepsilon(\%RH)}{d}$$

As seen in this equation, the reduction in area leads to a smaller capacitance and hence smaller sensitivity. Otherwise, the device properties stay the same. Furthermore, as mentioned before we have reached the limits in thickness for this type of polyimide (300Å) and any thinner devices are not reliable due to pinholes in the polyimide layer. To verify device operation, we have fabricated a set of devices with dimensions of 110μm x 110μm with the top electrode fingers having 10μm width and 10μm spacing, and another set with dimensions of 55μm x 55μm whose fingers are 5μm wide with a 5μm spacing.

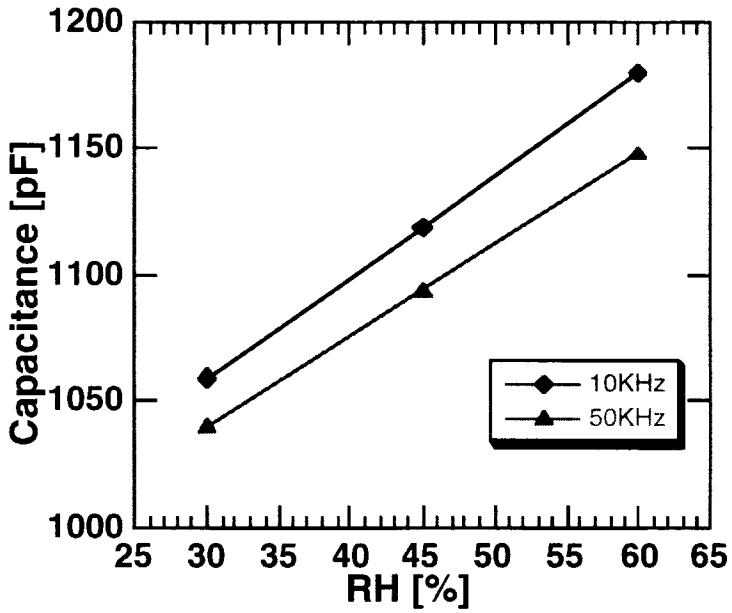

Figure 14: Measured capacitance vs. ambient RH for 2 different test frequencies for a 300Å-thick RH sensor mounted on an actual Silicon packaging substrate.

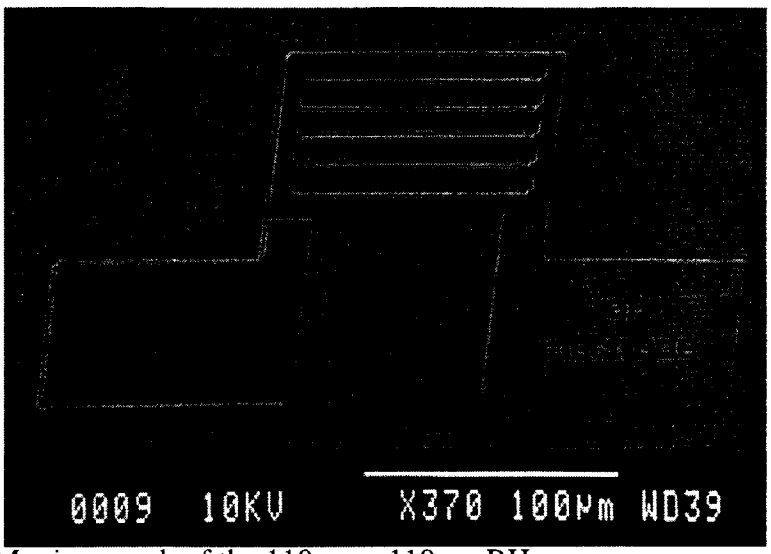

Figure 15: The SEM micrograph of the 110μm x 110μm RH sensor.

The SEM micrograph in Figure 15 shows one of these sensors (110μm x 110μm). Both designs have a linear response one of which (from the 110μm sensor) is shown in Figure 16. Therefore, one can realize smaller sensors at the expense of reduced sensitivity.

In summary, by using ultra-thin polyimide films, a highly sensitive polyimide humidity sensor has been realized with the highest sensitivity of 3.4pF/%RH for thinnest (300Å) devices. The output of the devices is very linear with a nonlinearity of less than a few percent RH. The sensors survive the anodic bonding process with a very high yield. The stability of the sensor in different moisture environments has been evaluated and the sensor is found to drift very little at moderate humidity levels. Scaling the device in area is possible at the expense of reduced sensitivity. Future work will focus on the application of these devices in animal experiments.

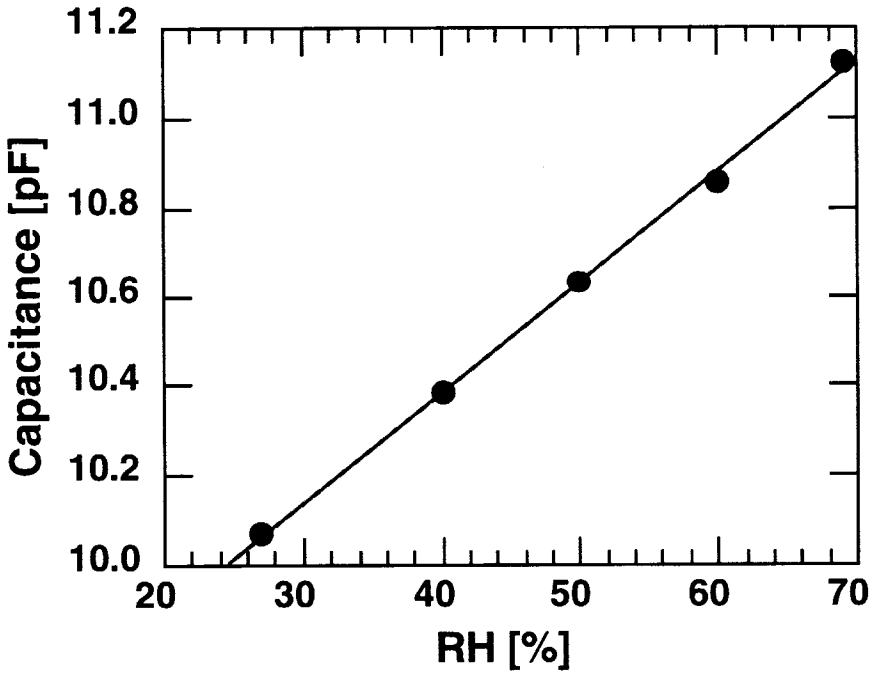

Figure 16: Measured capacitance vs. RH for the 110μm x 110μm RH sensor.

2.3 Low Profile Packaging: Si-Si Bonding using the Gold-Silicon Eutectic

The gold-silicon eutectic, with a melting temperature under atmospheric pressure of 363°C, is suitable for low temperature bonding applications. We are thus investigating this approach for alternative packaging of microstimulators. This section describes some of the progress made in this area.

In traditional approaches in Si to Si bonding using a eutectic gold-silicon intermediate layer, a Ti or Cr layer is deposited on the Si substrate below the gold layer, in order to promote adhesion, which is normally poor between gold and silicon. However, the Ti layer results in a higher melting temperature since silicidation must be reached first. Hence, in order to achieve bonding at a lower temperature, and since we believe that the feature size of our bonding area is large enough so that adhesion of gold on silicon may not be an issue, we decided, as a first attempt, to bond after direct deposition of gold on silicon.

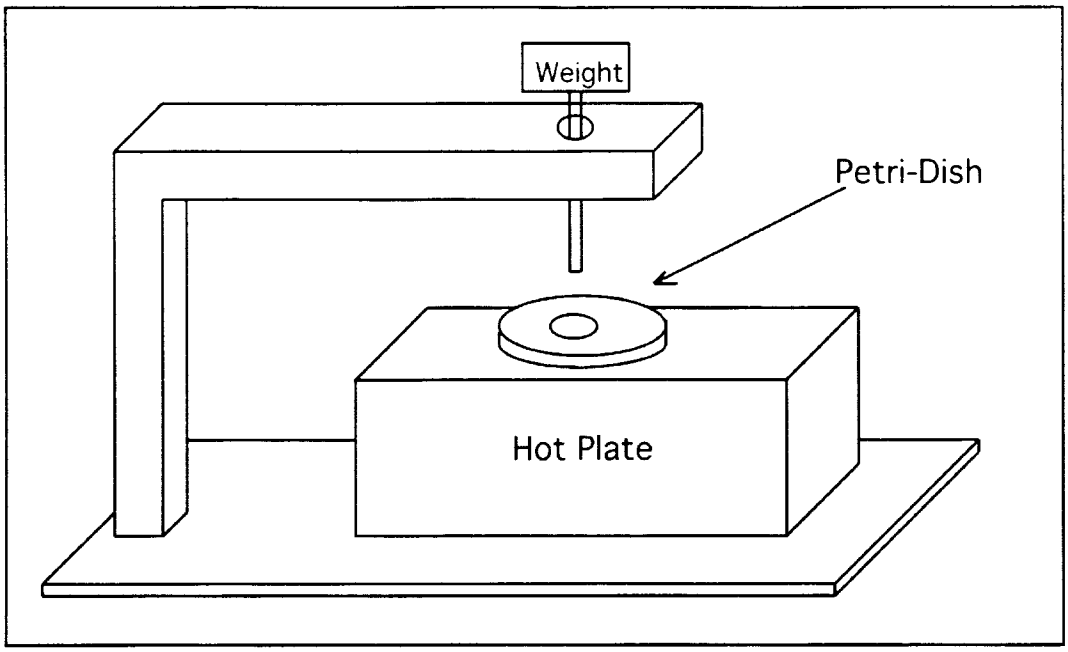

Figure 17: Bonding setup.

The first bonding attempts were made using the same setup as used for the anodic bonding. However, because of a need to have a better control over the temperature and the applied pressure, a specific bonding setup was designed as described in Figure 17. Using this setup the procedure is as follow: the two pieces to be bonded together are placed on the hot plate, a Petri-Dish with a hole is used to maintain temperature uniformity.

Some of the results obtained are described in Table 7. The silicon-gold wafers used have either a 1000Å or 2000Å thick sputtered or deposited gold layer. 1 cm^2 pieces were diced to be used for bonding. Attempts have been made with either 2 silicon-gold pieces or one silicon-gold and one bare silicon. As can be seen from Table 7, very few attempts have been successful in even getting a small bond (when achieved these bonds were not uniform across the bonding area), and, more surprisingly, were not reproducible. A possible explanation is the outdiffusion of Si through the gold layer, which has been reported in the literature and can take up to 6 weeks. However, we must verify this explanation; and we are currently conducting additional experiments and, a literature study, to improve our understanding of the bonding process.

2.4 Remote Monitoring of Humidity Inside the Package

In the previous progress reports, calculations and simulations of a system which could monitor dew point inside the package, were described. The underlying principle of the system relied on measuring the impedance of an external coil, which would reflect the change of the load of an internal coil coupled to a dew point sensor or a humidity sensor. For reasons due to stability and sensitivity of the measurements, it was found that this approach was not the most suitable one for our application. Hence a new approach has been developed and tested. As we will see in the following paragraphs, measurements have been made, which show the workability of this approach.

Table 7: Summary of eutectic bonding results.

Bond #	Type	Temp(°C)	Up t min	Time up	Down t min	Pressure	Comments	Pull test results
A4	2*Si-Au-(Cr,Ni)	500		1h15'		0	3 pairs.	0
		540		45'		Small	5 pairs. Acetone IPA cleaning.	0
A9	2*Si-Ti-2000Au	400		30'		Heavy	5 pairs each. Mirror-like surface after	0
		450		1h		(few kg's)	bonding.	0
A18-1	2*Si-2000Au	high		2h		Old setup	4 pairs. Acetone IPA cleaning. Remove weight before cooling.	0
A18-2	2*Si-2000Au	high		3h		"	1 pair. Acetone, IPA cleaning.	Razor blade
A18-3	2*Si-2000Au	high		2h40'		"	1 pair. Acetone, IPA cleaning.	Razor blade
A18-4	Si-2000Au/Si	high		2h40'		"	1 pair. Acetone, IPA cleaning.	0
A18-5	Si-2000Au/Si	high		3h		"	2 pairs. Acetone, IPA, BHF dip.	0
A18-6	2*Si-2000Au	540		10'		tweezers	1 pair.	++
A18-7	2*Si-2000Au	540	0	few'		tweezers	1 pair.	++
A18-8	2*Si-2000Au	540	0	few'		tweezers	4 pairs, 1 pair.	?, **300g**
A18-C1-1	Si-2000Au/Si	540	0	few'		tweezers	Go back on the hot plateafter cooling down.	++ and +++
		400						
A18-C1-2	Si-2000Au/Si	high	0	8'	7'	Old setup		0
C1	2*Si	500				0		0
From now on always use the digital hotplate and a Petri-Dish to maintain a uniform temperature								
A18-9	2*Si-2000Au	420	10'	12'		tweezers		
A18-10	2*Si-2000Au	420	10'	12'		tweezers		+
A18-11	2*Si-2000Au	420	10'	2h		0		+++
			-	12'		tweezers		
C10-1	2*Si-1000Au	420	10'	2h	30'	440g		0
C10-2	2*Si-1000Au	420	10'	10'	10'	830g	Put pressure with hands before ramp-up	0
C10-3	2*Si-1000Au	420	10'	-	-	0		**700g**
			-	2'	-	hand/tweezers		
			-	-	10'	0		
C10-4	2*Si-1000Au	420	10'	-	-	0		0
			-	3'	-	830g		
			-	-	20'	0		
C10-5	2*Si-1000Au	420	10'	10'	-	0		**550g**
			-	40''	-	830g+hands		
			-	-	20'	0		
C10-6	2*Si-1000Au	420	10'	10'	-	830g	No bond at all.	0
			-	2'	-	830g+hands		
			-	8'	20'	830g		
C10-7	2*Si-1000Au	420	10'	16'	-	830g		0
			-	1'	2'	830g+hands		
			-	-	20'	830g		
C10-8	Si-1000Au/Si	420	10'	35'	35'	830g		0
C10-9	Si-1000Au/Si	500	7'	30'	15'	830g	Apply pressure with hand before heating	0
C10-10	2*Si-1000Au	500	5'	45'	20'	830g		+
C10-11	2*Si-1000Au	420	10'	12'	20'	0		++
			-	45''		830g+hands		
C10-12	Si-1000Au/Si	420	10'	30'	20'	50g		++

0= no bond, += small adhesion, separates when moved, ++= sticks together but separated when applying small shear force, +++= sticks but separates when gluing for pull tests

The objective of the work described in this section is to develop a system, which will enable remote monitoring, in-vitro as well as in-vivo, of the amount of humidity inside the package. In this new approach, the sensor is a basic LC-tank, composed of a coil (which can be either discrete or integrated) attached to the humidity sensor described in the previous section. As the humidity inside the package changes, the capacitance C of the sensor varies and thus modifies the resonance frequency (f_o) of the sensor. This frequency, f_o, is measured using a simple inductor (a few turn wired coil, which acts as an antenna). When the antenna is placed in the vicinity of the sensor, its phase, measured over a wide range of frequencies using a gain-phase analyzer, exhibits a "dip" at the resonance frequency of the sensor. By measuring the position of this dip, we get the resonance frequency of the sensor and calculate the capacitance of the humidity sensor, which in its turn relates to the humidity inside the package.

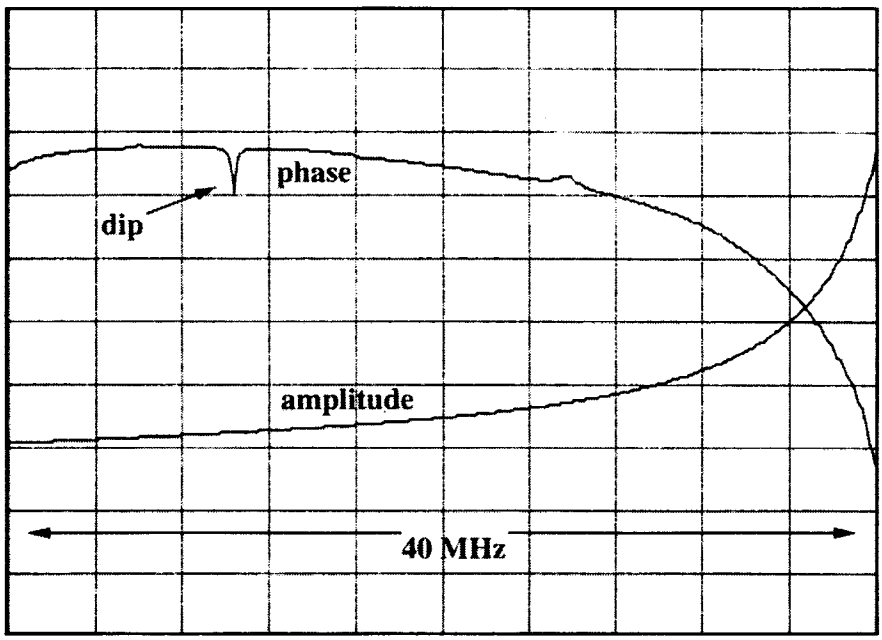

Figure 18: Impedance at the antenna.

In order to study how this approach can be utilized in our applications, some measurements were made using a pseudo-sensor. This pseudo-sensor is made of a discrete commercial inductive coil of 1μH (which corresponds to an inductance comparable to that we can obtain using a discrete coil small enough to fit inside the package or an integrated coil) attached to a discrete capacitor which simulates the humidity sensor. This pseudo-sensor was placed inside an antenna (a discrete wired coil made of 4 turns with a diameter of 9cm). The impedance of the antenna is measured using a gain-phase analyzer, over a wide frequency range first in order to detect the phase dip, then over a narrow range to isolate the dip more precisely. Figure 18 shows the gain-phase diagram obtained, and Figure 19 zooms in the dip area. Figure 19 was obtained using a sensor with a capacitance C=220pF. The calculated resonance frequency is $f_o=1/(2\pi\sqrt{LC})=11.290$ MHz. The value measured directly from the sensor gives $f_o=11.260$ MHz and the one obtained from the telemetry measurement is $f_o=11.267$ MHz. There is a good agreement between the calculated and measured values.

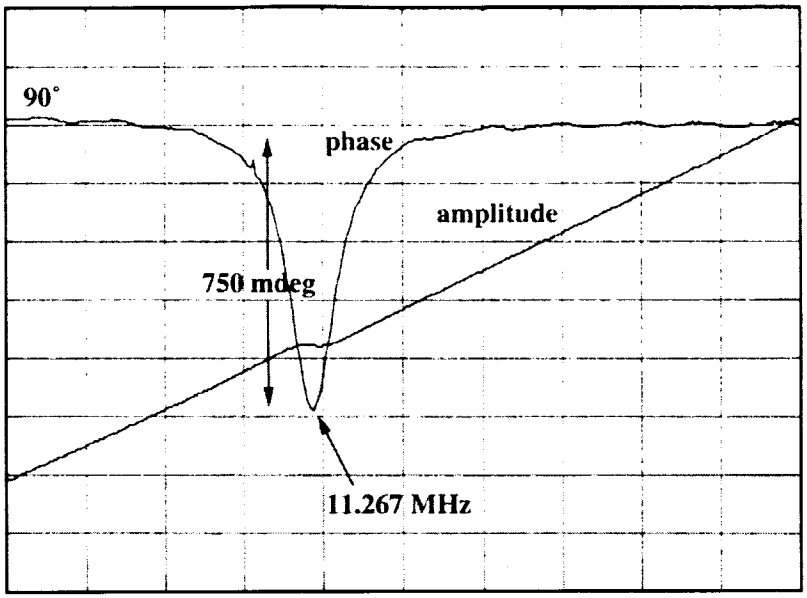

Figure 19: Exploded view of the dip area.

In order for this approach to be used in our application, the frequency shift from the variation of humidity inside the package must be large enough to be detectable. Using relative humidity vs. capacitance measurements described in the previous section, we simulated a change in humidity by varying the capacitance C of our pseudo-sensor. Table 8 summarizes the experimental results and Figure 20 shows the movement of the phase dip when the capacitance is varying from 260pF to 320pF, which corresponds to a humidity change from 20%RH to 80%RH when using a 1200Å thick polyimide humidity sensor. We see that in this case a 60% change in humidity corresponds to an approximate 1MHz change in the resonance frequency. This change is large enough to be easily detectable. Figure 21 shows the measured frequency vs. the corresponding relative humidity.

Table 8: Variation in the pseudo-sensor capacitance corresponding to humidity changes.

Capacitance	Corresponding humidity	Directly measured f_o	Telemetry measured f_o
260 pF	20%RH	10.436 MHz	10.444 MHz
270 pF	30%RH	10.244 MHz	10.280 MHz
280 pF	40%RH	10.092 MHz	10.116 MHz
290 pF	50%RH	9.904 MHz	9.896 MHz
300 pF	60%RH	9.728 MHz	9.716 MHz
310 pF	70%RH	9.580 MHz	9.584 MHz
320 pF	80%RH	9.440 MHz	9.428 MHz

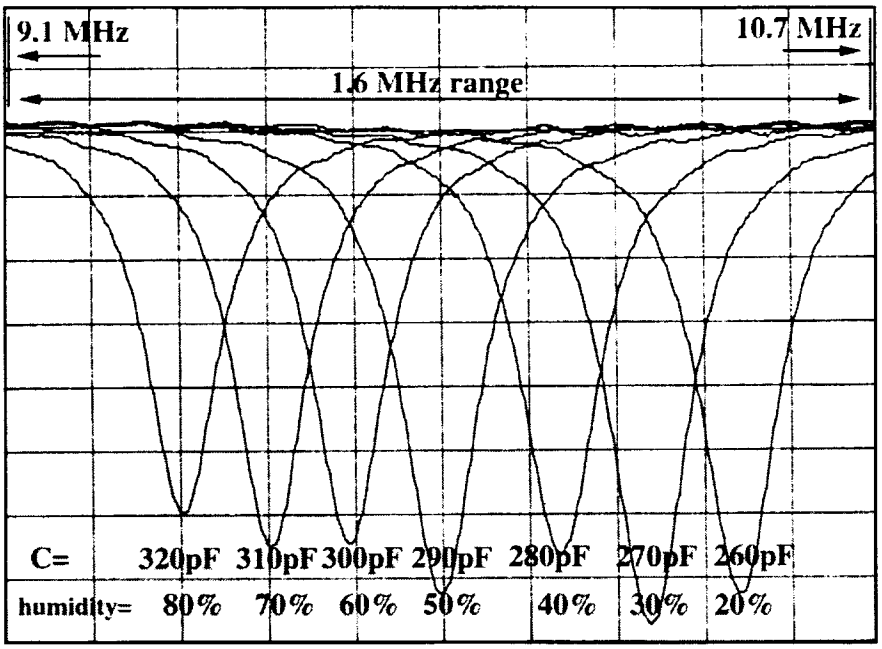

Figure 20: Variation of the capacitance of the pseudo-sensor corresponding to a humidity change.

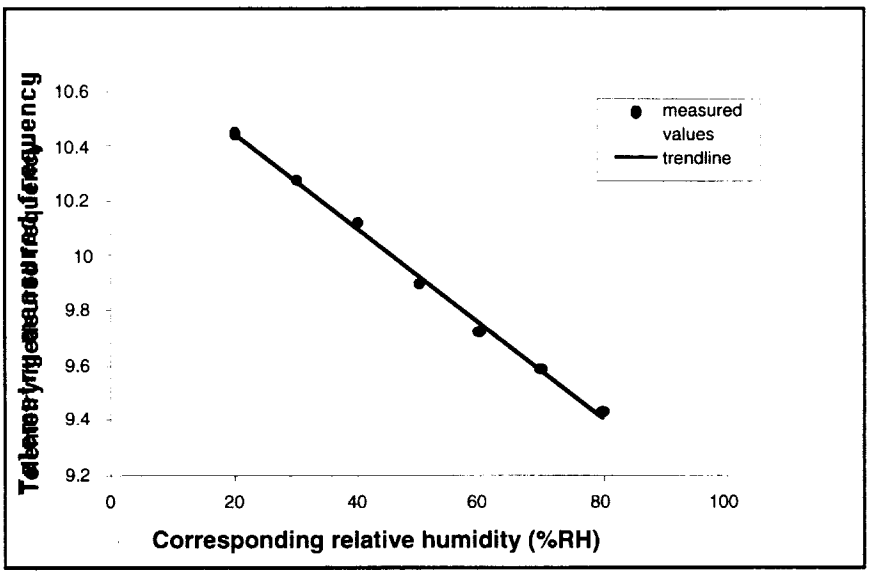

Figure 21: Resonance frequency vs. corresponding %RH for the pseudo-sensor.

Furthermore, the obtained resonance frequency should be independent of the position of the sensor relative to the antenna, or the angle between the sensor and the antenna coils. In Figure 22, the sensor is moved from the center of the coil (position A) towards the edges (B and C correspond to 1/3 and 2/3 of the radius from the center respectively). We see that the sensitivity increases but the obtained frequency does not change. In Figure 23, we vary the angle θ between the sensor and the antenna coils, from 0° (position A, parallel axes) to approximately 30°, 60° and

90° (positions B, C and D respectively, 90° corresponding to perpendicular axes, at which the coupling disappears). Once again, the sensitivity decreases due to a decrease in the coupling but the obtained resonance frequency remains the same.

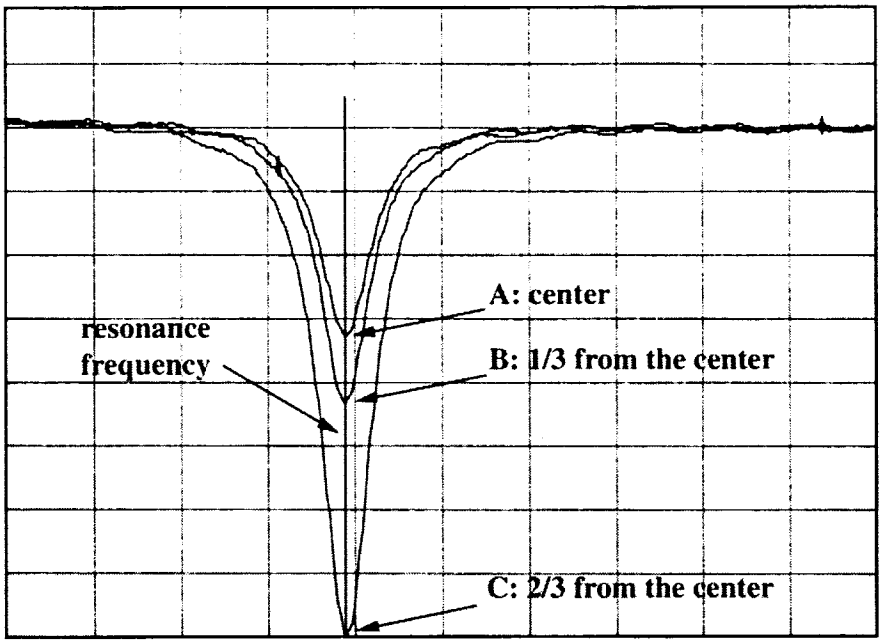

Figure 22: Influence of the position of the sensor relative to the antenna.

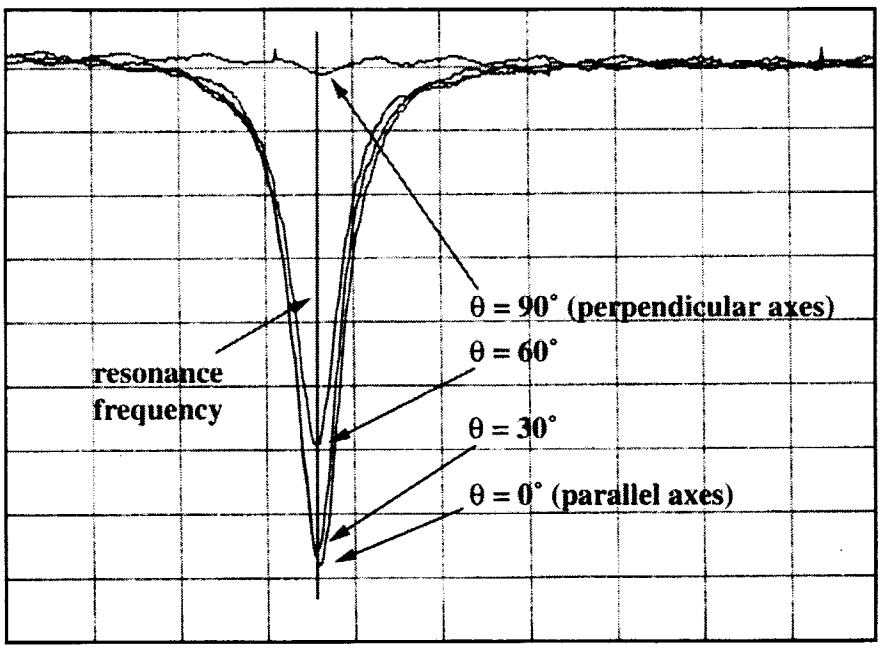

Figure 23: Influence of the angle θ between the sensor and antenna coils axes.

Finally, it should be noted that sensitivity can be increased by optimizing the antenna parameters, which are mainly the material of the wire, the diameter and the number of turns of the coil. A modification of the antenna (as long as we stay in the inductive range) does not change the position of the dip, only its magnitude.

In conclusion, we now have all the ingredients to apply the described measurements to telemetrically monitor humidity from implanted packages. This can be used in the testing of individually soaked packages, as well as to the batch testing of packages that would be bonded at a wafer level. The latter would allow us to monitor continuously and accurately the integrity of a large number of packages. This method should also allow us to monitor the behavior of packages implanted in vivo during the implantation period. We are planning to have packages equipped with the telemetry monitoring system in the coming quarter.

3. PLANS FOR THE COMING QUARTER

In the coming quarter we will continue working on the different areas described in the previous sections. We now have developed a reliable method to monitor the humidity inside the package telemetrically, which will be implemented with an actual humidity sensor and a coil that can be mounted into the packages. These packages will be used either for accelerated in-vitro studies or for animal implants. We will also continue our efforts in low-profile silicon to silicon bonding.

References

[1] T. Boltshauser, L. Chandran, H. Baltes, F. Bose and D. Steiner, "High Sensitivity CMOS Humidity Sensors With On-chip Absolute Capacitance Measurement System", *Sensors and Actuators B*, pp. 75-80, Vols. 15-16, 1993.